

Supporting Information

Polyphenol-assisted assembly of Au-deposited polylactic acid microneedles for SERS sensing and antibacterial photodynamic therapy

Zi-Chun Chia^{a‡}, Yi-Lun Chen^b, Cheng-Hsun Chuang^b, Chou-Hsun Hsieh^b, Ya-Jyun Chen^a, Kuan-Hsu Chen^a, Tzu-Chi Huang^a, Mei-Chin Chen^{b*}, and Chih-Chia Huang^{a, c*}

^a Department of Photonics, National Cheng Kung University, Tainan 70101, Taiwan.

^b Department of Chemical Engineering, National Cheng Kung University, Tainan 70101, Taiwan.

^c Center of Applied Nanomedicine, National Cheng Kung University, Tainan 70101, Taiwan.

*corresponding author

Email address: kokola@mail.ncku.edu.tw , c2huang@email.ncku.edu.tw

Experimental Section

Chemicals and Materials

Hydrogen tetrachloroaurate (III) trihydrate ($\text{HAuCl}_4 \cdot 3\text{H}_2\text{O}$, 99%), tannic acid (TNA), 3-(4,5-Dimethylthiazol-2-yl)-2,5-diphenyltetrazolium bromide (MTT assay reagent), methylene blue (MB) were obtained from Alfa Aesar. Luria-Bertani (LB) broth and phosphate-buffered saline (PBS, pH 7.0) were purchased from Athena ES and Thermo. Dulbecco's modification of Eagle's medium (DMEM) and Roswell Park Memorial Institute (RPMI) medium were obtained from Corning. Rhodamine 6G (R6G), 9,10-anthracene-nediy-bis(methylene)dimalonic acid (ABDA), and uric acid were purchased from Sigma-Aldrich. Cell counting kit 8 (CCK8) was obtained from Dojindo Laboratories. Guanine, xanthine, and hypoxanthine were purchased from Acros Organics. Agar and Tryptic soy broth (TSB) were obtained from Amresco and Neogen, respectively. Polydimethylsiloxane (PDMS, Sylgard 184) and polylactic acid (PLA) were purchased from Dow Corning and Flmt Corp, respectively. Aqueous solutions were prepared using deionized water.

Characterization

The micro-structures of MN arrays and nanoparticle images were verified using scanning electron microscopy (SEM, JSM-6700F) at ten keV. The absorption spectra were recorded using an ultraviolet-visible spectrophotometer (UV-vis, JASCO V-730) and a microplate reader (BioTek/SYNERGY-H1). The laser power transmittances of different wavelengths were measured using a photodiode power sensor (Thorlabs). The crystalline structure of Au NPs was characterized by X-ray thin-film diffractometer (XRD, Rigaku). The chemical states of Au NPs on AuMNs were identified by X-ray photoelectron spectroscopy (XPS, Thermo Fisher Scientific ESCLAB Xi⁺). The concentrations of Au were quantified by atomic absorption spectroscopy (AAS, SensAA GBC). The average particle diameters of Au NPs were calculated using SigmaScan software and the coverage ratio of Au NPs were calculated using ImageJ software.

ESR spectroscopy (Bruker, ELEXSYS E-580) was used to confirm singlet oxygen generation. 100 μL of singlet oxygen spin trapper 2,2,6,6-tetramethylpiperidine (TEMP) at 10 mM was dropped on AuMNs-MB_[16 ppm], and subsequently irradiated with 650 nm-excitation at 75 mW for 20 min. Afterward, TEMP solution was removed from AuMNs-MB_[16 ppm] and was added into 900 μL deionized water. Thus, ESR spectra of TEMP solution (final concentration 1 mM) were recorded and normalized. ESR conditions were as follows: microwave power 15 mW, modulation amplitude 0.16 T, modulation frequency 100 kHz, sampling time 0.02 s.

Fabrication of transparent PLA MNs

A stainless steel master structure of MNs was obtained from Hong-Da Precision Industry Co., Ltd. (New Taipei City, Taiwan). Female MN molds made of PDMS were fabricated by inversely replicating metallic master structures precisely. These PDMS molds were repeatedly used to make

the PLA MN patch. The optically transparent PLA MNs were prepared using a vacuum molding process. PLA filaments (a length of 1.7 cm, six filaments for each mold) were added onto the PDMS mold surface and then placed into a vacuum oven, set at one inHg and 190 °C for one h. After breaking the vacuum, a glass petri dish was placed onto the surface of the filled mold at 190 °C for 1 h to make the patch flat. Subsequently, the mold was put into an ice bath for 5 min to prevent recrystallization of PLA and form a transparent PLA patch. Finally, the fabricated PLA MNs were gently peeled from the mold.

Preparation of SERS-active AuMNs

PLA MNs were immersed in a TNA solution (5 mM) for 10 min at room temperature and then were dried by placing them upside-down in the heating oven at 50 °C for 20 min. Afterward, 100 µL of H₂AuCl₄ (5 mM) was added to the MNs, with an upside-down drying process at 50 °C. After repeating the step of adding H₂AuCl₄ with the same volume and concentration twice, the MNs were dried at 50 °C with an upside-down drying process for 20 min. Finally, the SERS-active AuMNs with red tips were obtained.

Preparation of SERS/PDT-active AuMNs-MB

Firstly, with the upside-down drying process, 100 µL of MB solution (16 ppm) was added to AuMNs while drying in the heating oven at 50 °C for 20 min. Then, the SERS/PDT active AuMNs-MB with violet-blue tips were obtained.

Preparation of AuMNs-R6G

Firstly, with the upside-down drying process, 100 µL of R6G solution (48 ppm) was added to AuMNs while drying in the heating oven at 50 °C for 20 min. Then, AuMNs-R6G with red tips were obtained.

Preparation of ascorbic acid-synthesized AuMNs and NaBH₄-synthesized AuMNs

100 µL of mixture containing H₂AuCl₄ (5 mM) and the reductant ascorbic acid (5 mM) was added to PLA MNs. The MN were subjected to an upside-down drying process at 50 °C. This step was repeated twice with the same volume and concentration of the mixture. Finally, the MNs were dried at 50 °C with an upside-down drying process for 20 min, resulting in the formation of ascorbic acid-synthesized AuMNs with red tips. To prepare NaBH₄-synthesized AuMNs, the same steps and concentration were used, but ascorbic acid was replaced with NaBH₄.

SERS measurement and calculations of analytical enhanced factor (AEF)

SERS spectra were acquired on a Jobin–Yvon LabRAM high-resolution micro-Raman spectrometer (Horiba iHR 320) using 785/633 nm laser excitation (DPSSL Driver II) with a power of 5 mW and a diameter of 2.88 µm², and were integrated into an Olympus BX53 microscope with ×20 objective lens. Each raw spectrum (400-1700 cm⁻¹) was employed with an integration time of 10 s and was baseline corrected to remove the fluorescence background. For the detection of aqueous analytes, AuMNs were covered by aqueous samples with desired concentration; then, the SERS spectra were subsequently acquired by 785 nm excitation for MB and purines-based molecules and 633

nm excitation for R6G. To detect dried analytes, AuMNs were covered by 100 μL of aqueous samples with desired concentration and dried at 50 $^{\circ}\text{C}$ for 20 min with an upside-down drying process. The SERS spectra were subsequently acquired by 785 nm excitation for MB and purine-based molecules and 633 nm excitation for R6G. The SERS mapping images of a single MN tip were obtained for 10 \times 10 pixels within 350 \times 350 μm^2 field at 2s acquisition with \times 20 objective lens. The 3D reconstruction images were built by serial images in the z-direction. The SERS mapping image within 3 \times 3 microneedles region was obtained for 10 \times 10 pixels within 3000 \times 3000 μm^2 field at 1s acquisition with \times 20 objective lens.

The values of AEF were obtained experimentally using the following equation:

$$\text{AEF} = \frac{I_{\text{SERS}} \times C_{\text{Raman}}}{C_{\text{SERS}} \times I_{\text{Raman}}}$$

I_{SERS} is the SERS intensity of analytes with AuMNs, I_{Raman} is the SERS intensity of pure analytes, C_{SERS} is the concentration of analytes with AuMNs, and C_{Raman} is the concentration of pure analytes.

Fluorescence imaging

The cross-sectional fluorescent images of a single MN tip of AuMNs with dried MB (16 ppm) and R6G (48 ppm) were obtained using confocal fluorescent microscopy (Olympus IX73) with 532 nm laser excitation at \times 20 magnification. Each image was acquired for 512 pixels within a 350 \times 350 μm^2 field at 20 ms acquisition. The 3D reconstruction images were built by serial images in the z-direction.

Bacterial cultivation and SERS-based detection

The gram-positive *Staphylococcus aureus* ATCC 25922 (*S. aureus*) bacteria were cultured in tryptic soy broth (TSB) at 200 rpm/min and 37 $^{\circ}\text{C}$ overnight. The bacteria cells were centrifuged at 8500 rpm/min three times and resuspended in phosphate-buffered saline (PBS, pH 7.4). The optical density at 600 nm (OD_{600}) of bacteria suspension was measured on a microplate reader (BioTek/SYNERGY-H1) to determine bacterial cell growth. To determine bacteria within the agarose skin phantom, the bacterial suspension was first incubated in PBS for 6 hours at 37 $^{\circ}\text{C}$. Next, 200 μL of the bacterial suspension at the desired concentration was combined with 1800 μL of LB agar in a 3.5 cm dish. The agarose skin phantom was allowed to solidify for 12 hours before use. An AuMN was then introduced into the agarose skin phantom containing bacterial colonies, and SERS spectra were collected using 785 nm backside-excitation. For SERS measurement of bacteria adhered to the surface of the agarose skin phantom, 100 μL of the bacterial suspension at the desired concentration was applied to an as-solidified LB agar surface. After incubating for 12 hours, an AuMN was introduced into the agarose skin phantom containing superficial bacterial colonies, and SERS spectra were collected using 785 nm backside-excitation.

Antibacterial photodynamic assay

The 1×10^4 CFU/mL of bacteria suspensions were plated on the agarose skin phantom. To evaluate

the antibacterial effect of different MNs, PLA MNs, AuMNs, and AuMNs-MB_[16 ppm] were inserted into the agarose skin phantom without irradiation, respectively. To assess the antibacterial effect of varying irradiation time, AuMNs-MB_[16 ppm] were inserted into the agarose skin phantom with 0, 1, 5, 10, and 20 min of 650 nm backside excitation (75 mW), respectively. The microneedles were removed after irradiation. To determine the antibacterial effect of three PDT cycle, AuMNs-MB_[16 ppm] groups with lower laser excitation energy (50 mW for 20 min, 75 mW for 8 min, and 25 mW for 20 min) were performed. After completion of one PDT, same AuMNs-MB_[16 ppm] were reinserted into another agarose skin phantom and proceed PDT again. A total of three cycle of PDT were performed.

The area percentages of bacteria colonies were calculated and normalized using ImageJ software after 24 hr of incubation at 37 °C. The area percentages of bacteria colonies were obtained using the following equation:

$$\text{Colony area percentage} = \frac{A_{\text{experiment}} \times A_{\text{MN}}}{A_{\text{MN}} \times A_{\text{control}}} \times 100\%$$

$A_{\text{experiment}}$ is the total area of colonies in each experiment group, A_{MN} is the area of microneedles array, A_{control} is the total area of colonies in control group.

Singlet oxygen measurement

ABDA was used to measure singlet oxygen generation. Briefly, 200 μL of ABDA (51.3 ppm) was dropped onto AuMNs-MB_[16 ppm], then the absorbance of ABDA aliquot was measured every 2 min of 650 nm irradiation at 75 mW.

Cytotoxicity assay

The human monocytic cell line (THP-1) and mouse embryonic fibroblasts cell line (3T3) were cultured at 10^5 cells with MNs, AuMNs, and AuMNs-MB, respectively. After 24 or 48 hr incubation, 20 μL of CCK-8 reagent was added to 180 μL of cells, followed by a 2 hr incubation. The absorbance determined the cell viability at 450 nm.

Table S1. SERS measurement conditions and AEF value of each analyte.

Analytes	Laser wavelength	Power	Peak	AEF for aqueous analytes	AEF for dried analytes
Adenine	785 nm	5 mW	735 cm^{-1}	2.86×10^3	3.19×10^4
MB	785 nm	5 mW	446 cm^{-1}	1.58×10^3	2.12×10^4
R6G	633 nm	5 mW	1507 cm^{-1}	1.96×10^3	3.88×10^4

Table S2. The calculated average particle size and coverage ratio of Au NPs on AuMNs synthesized with different concentrations of TNA.

TNA concentration	Particle diameter	Coverage ratio
1 mM	61.2 ± 14.6 nm	7.1 %
3 mM	89.0 ± 30.9 nm	40.6 %
5 mM	135.4 ± 22.9 nm	69.1 %

Table S3. The calculated average particle size and coverage ratio of Au NPs on AuMNs synthesized with different concentrations of HAuCl_4 .

HAuCl_4 concentration	Particle diameter	Coverage ratio
1 mM	60.5 ± 16.8 nm	11.2 %
3 mM	78.8 ± 15.2 nm	49.9 %
5 mM	135.4 ± 22.9 nm	69.1 %

Fig. S1a shows the XRD pattern of AuMNs with diffraction peaks at 38.1 °, 44.3 °, 64.6 °, 77.6 °, and 81.7 °, which corresponds to the (111), (200), (220), (311), (222) planes, respectively, of face-centered cubic (fcc) structured Au (JCPDS no. 04-0784). The XPS spectrum in Fig. S1b presented the $4f_{5/2}$ at 87.7 eV and Au $4f_{7/2}$ at 84.0 eV of Au material.¹

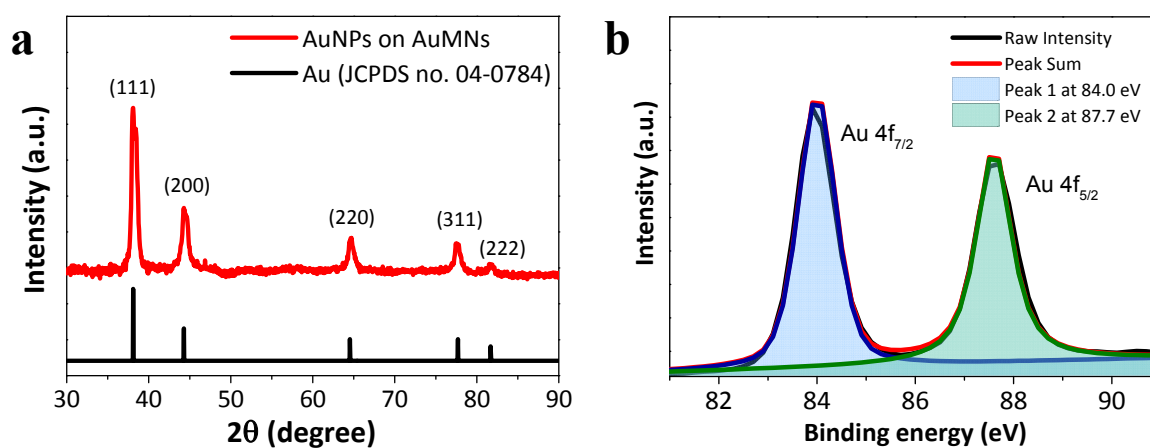


Fig. S1 (a) XRD patterns of Au NPs on AuMNs and the standard Au (JCPDS no. 04-0784). (b) Au 4f orbitals in XPS spectra of the AuMNs.

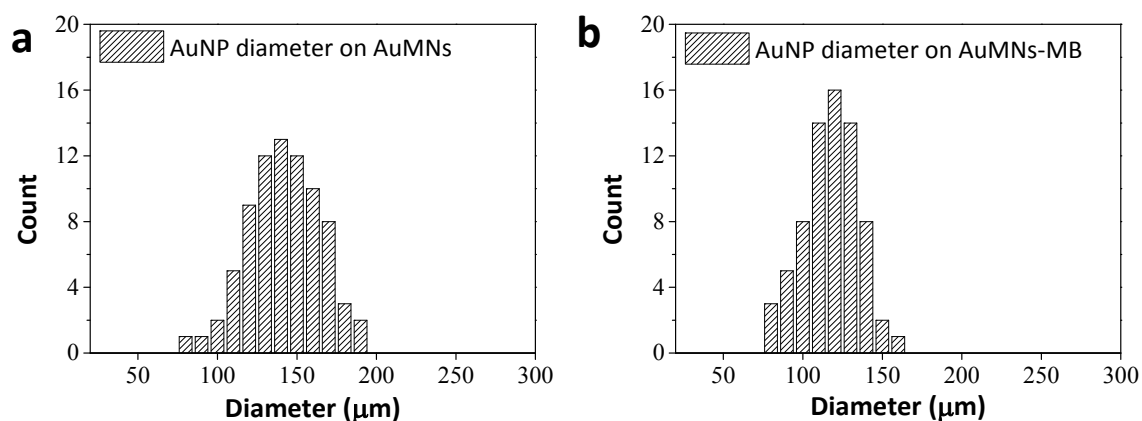


Fig. S2 Particle distribution of AuNPs on a single tip of (a) AuMN and (b) AuMN-MB from SEM images.

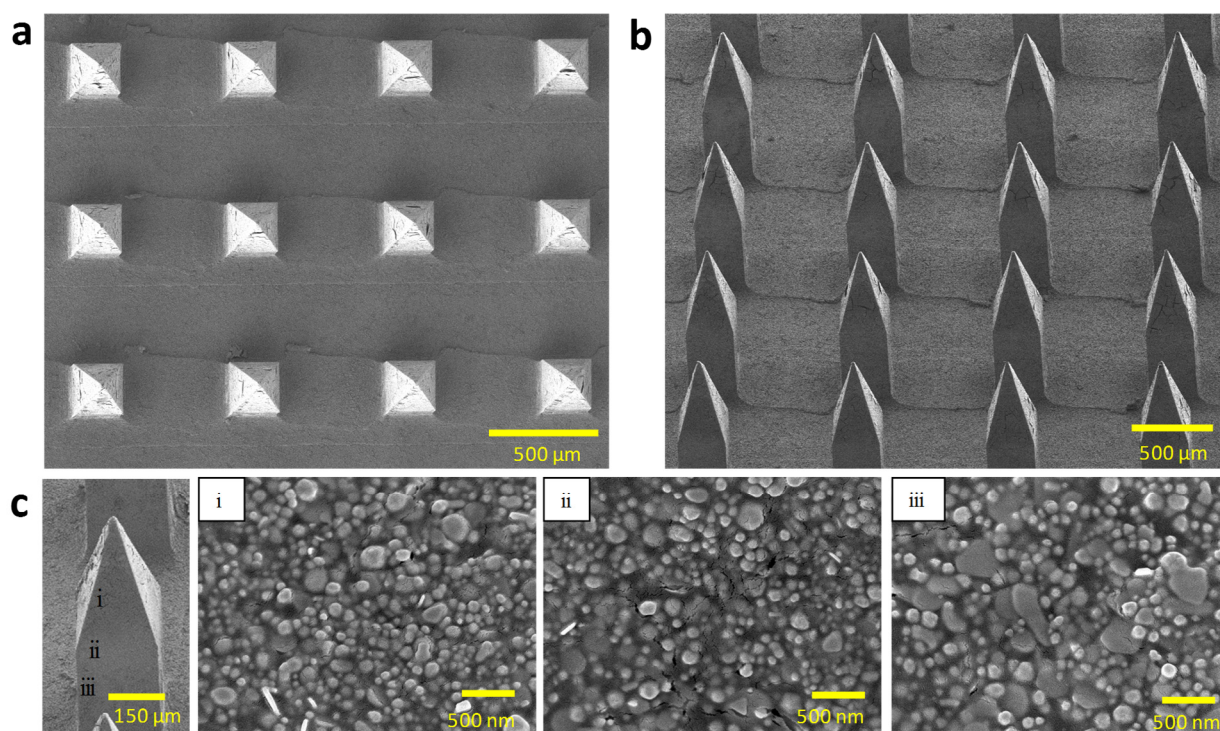


Fig. S3 SEM image of AuMNs within (a) 3x4 (top view) and (b) 4x4 (60° tilt angle) microneedles. (c) SEM image of AuNPs on the single microneedle's surface at the (i) tip, (ii) upper site of body, and (iii) lower site of body.

To compare the coating adhesion of Au-deposited microneedles synthesized using TNA with those synthesized using ascorbic acid or NaBH₄ reductant, the SEM images and solid-state UV-visible absorption spectra of the samples before and after insertion into pigskin were conducted. The results of both evaluations demonstrated that the Au coating was still on the TNA-synthesized AuMN surface after insertion into the pigskin (Fig. S4a and S5a). In contrast, the Au NPs were notably separated from the tip of MNs after skin insertion for the ascorbic acid and NaBH₄ groups, according to the SEM images (Fig. S4b and S4c) and solid-state UV-visible absorption spectrum (Fig. S5b and S5c). These results demonstrated a strong interfacial interaction between Au@TNA and PLA@TNA MNs via TNA linkage.

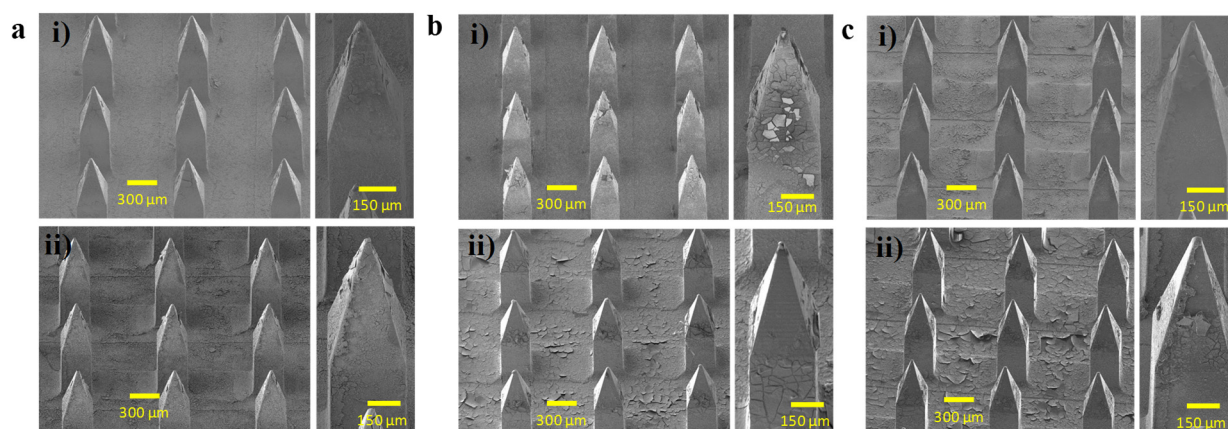


Fig.S4 SEM images of (a) TNA-, (b) NaBH₄-, and (c) ascorbic acid-synthesized AuMNs (i) before and (ii) after puncturing into pigskin.

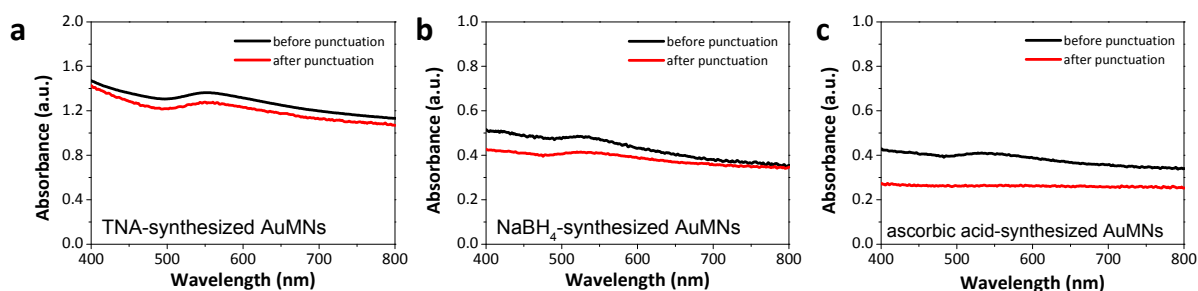


Fig.S5 Absorption spectrum of (a) TNA-, (b) NaBH₄-, and (c) ascorbic acid-synthesized AuMNs before (black) and after (red) puncturing into pigskin.

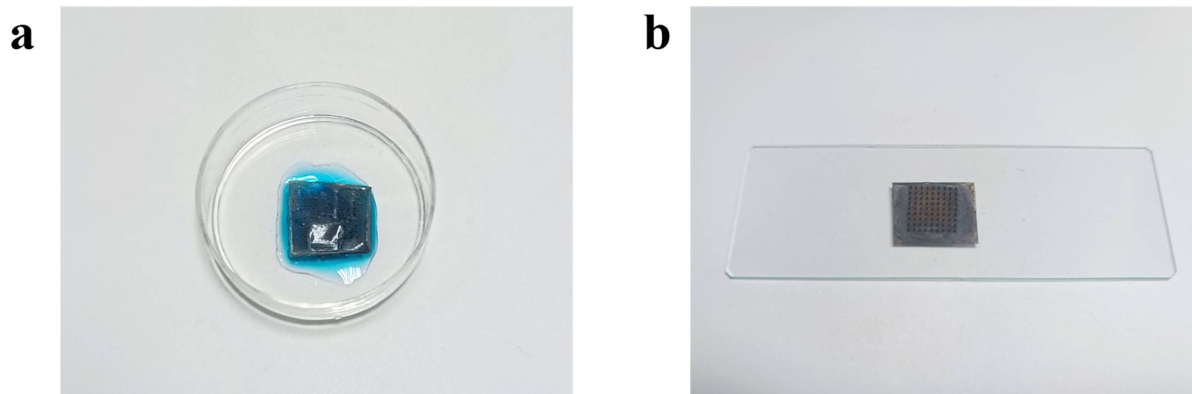


Fig. S6 Photographs of AuMN with (a) aqueous and (b) dried analytes for SERS measurement.

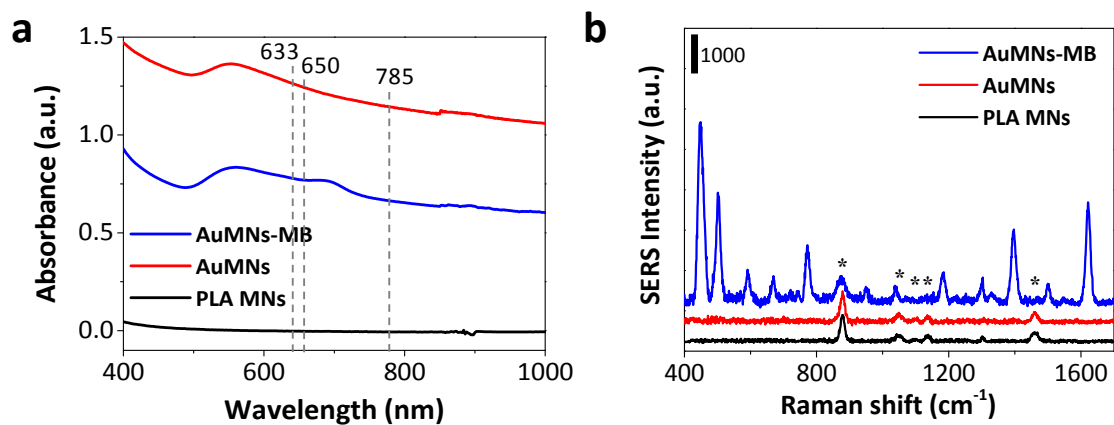


Fig. S7 (a) UV-Vis absorption spectra and (b) SERS spectra of PLA MNs, AuMNs, and AuMN-MB_[16 ppm]. (* labels represent the Raman characteristic peak of PLA)

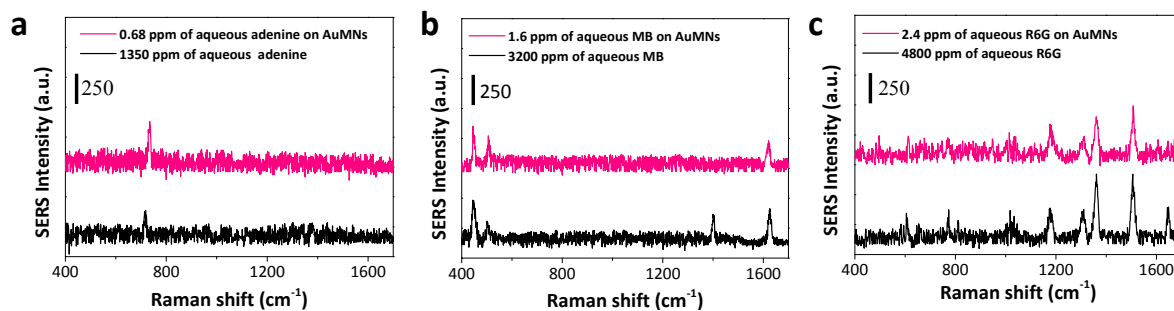


Fig. S8 SERS spectra of aqueous (a) adenine, (b) MB, and (c) R6G on AuMNs compared to the Raman spectra of aqueous (a) adenine, (b) MB, and (c) R6G alone

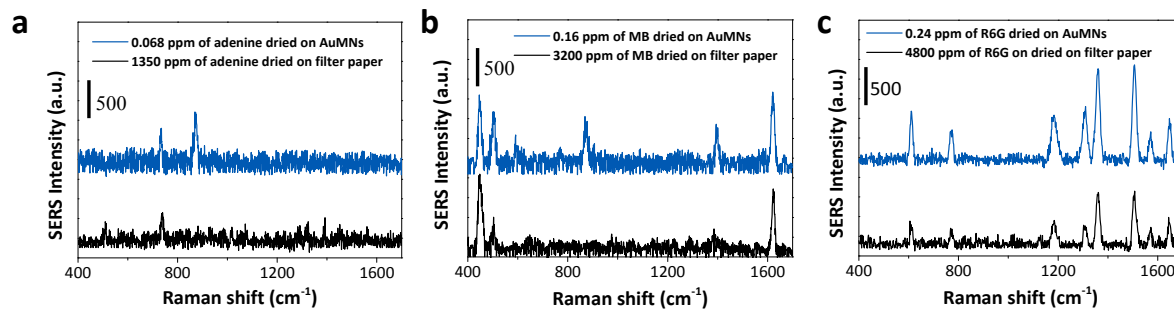


Fig. S9 SERS spectra of (a) adenine, (b) MB, and (c) R6G dried on AuMNs compared to the Raman spectra of (a) adenine, (b) MB, and (c) R6G dried on blank filter paper.

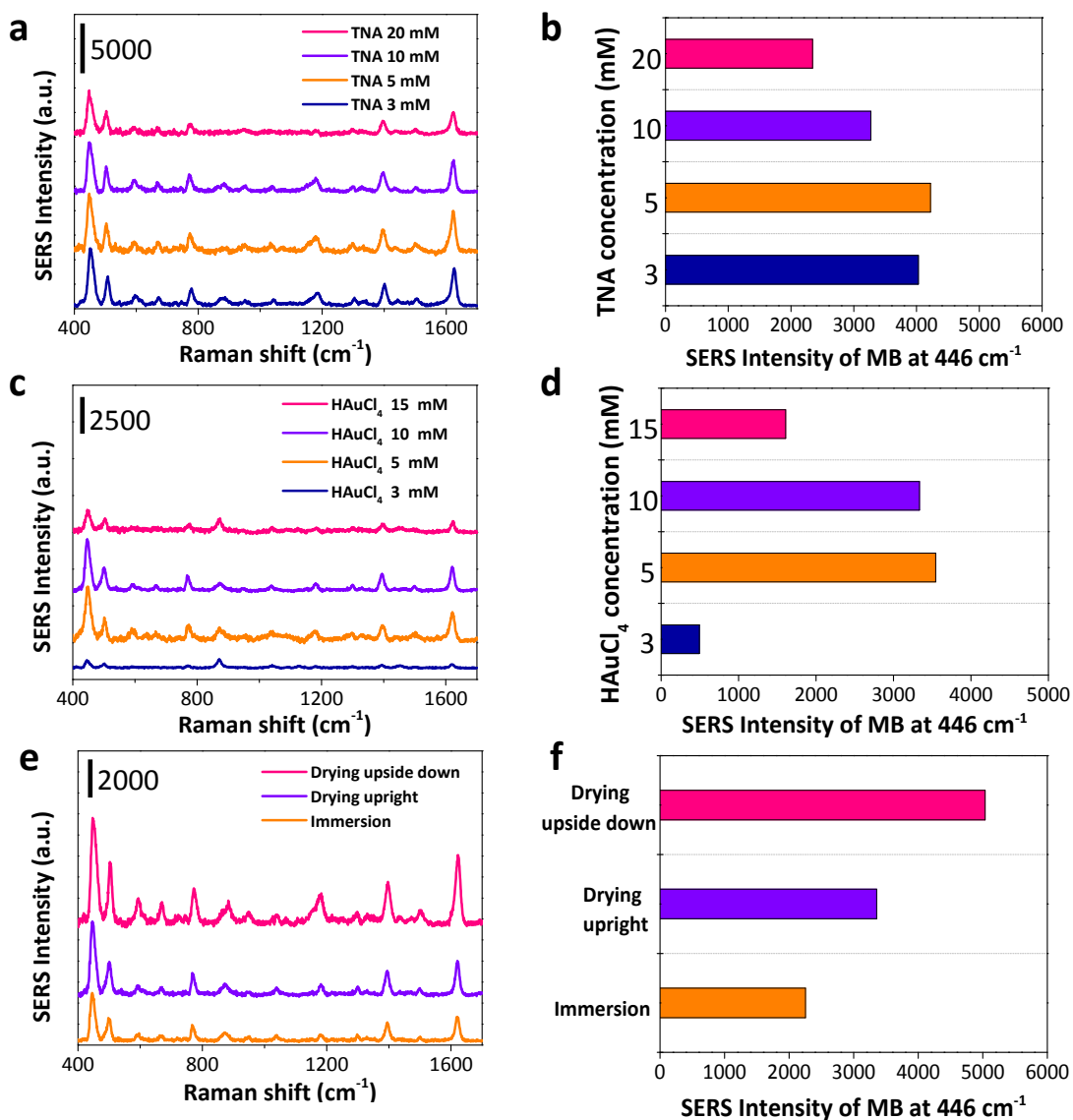


Fig.S10 SERS spectrum of AuMNs-MB_[16 ppm] with optimal concentrations of (a) TNA, (c) HAuCl₄, and (e) different synthesis methods. The corresponding histogram of SERS intensity from (b) a, (d) c, and (f) e.

As the TNA concentrations decreased below 5 mM, the size of the Au NPs decreased from 135.4 ± 22.9 nm at 5 mM of TNA to 61.2 ± 14.6 nm at 1 mM of TNA (Table S2, Fig. S11a-c). This is likely due to a decrease in HAuCl_4 concentrations below 5 mM, leading to the generation of fewer Au(0) atoms and failed growth of larger particle size. SEM images were analyzed using ImageJ to determine the coverage ratio (by counting the light dot area from the substrate area), which indicates that the coverage ratios of 1 mM and 3 mM TNA were lower than 5 mM TNA. The measurement results are summarized in Table S2. Consistently, the AuMNs presented a significant absorption band at ~ 560 nm of AuMNs at 5 mM TNA, which is higher than 1 mM and 3 mM TNA (Fig. S11d), indicating the greater production of AuNPs at 5 mM TNA.

We also fabricated AuMNs using HAuCl_4 concentrations ranging from 1 mM to 5 mM. The SEM images showed an increase in particle concentrations and sizes as the HAuCl_4 concentrations increased from 1 mM and 5 mM (Fig. S12a-c). These results are summarized in Table S3. A significant absorption band of the AuMNs using 5 mM HAuCl_4 at ~ 560 nm was shown, while the absorption band of the AuMNs decreased at 1 mM and 3 mM HAuCl_4 .

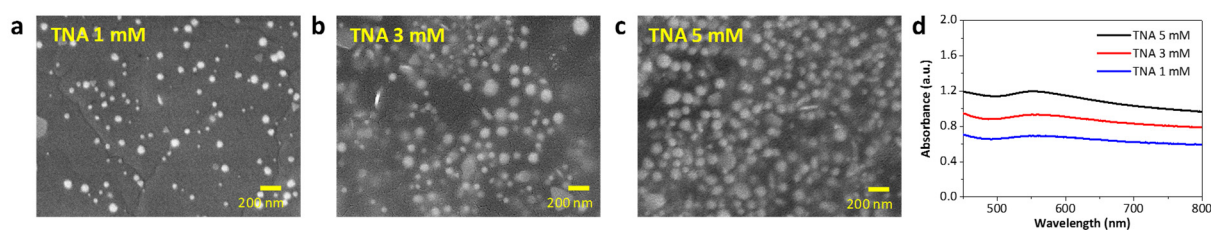


Fig. S11 SEM images of Au NPs on AuMNs synthesized using (a) 1 mM, (b) 3 mM, (c) 5 mM of tannic acid (TNA), and the corresponding (d) absorption spectra.

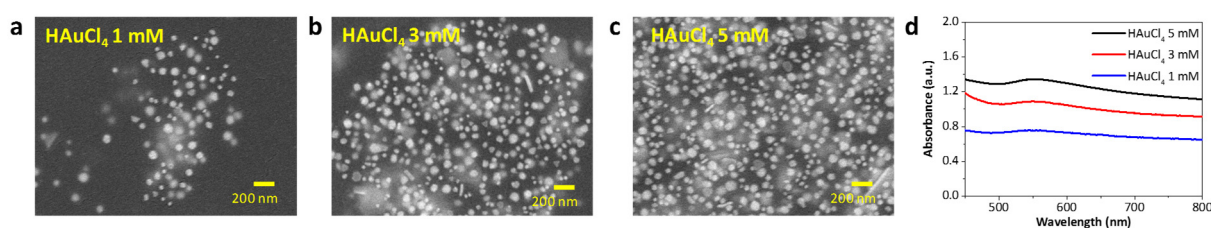


Fig. S12 SEM images of Au NPs on AuMNs synthesized using (a) 3 mM, (b) 5 mM, (c) 10 mM of HAuCl_4 , and the corresponding (d) absorption spectra.

As subjected to 10x object (lack of z-focusing), AuMNs exhibited high SERS signal reproducibility with an 8.3% relative standard deviation (RSD) that was revealed by 20 spectra of MB-related characteristic peaks generated from individual tips through tip-by-tip measurements (Fig. S14)

As subjected to 20x object (z-focusing), the SERS signal uniformity within 3×3 microneedles of AuMNs_[16 ppm] at each z-focusing height were measured (Fig. S15).

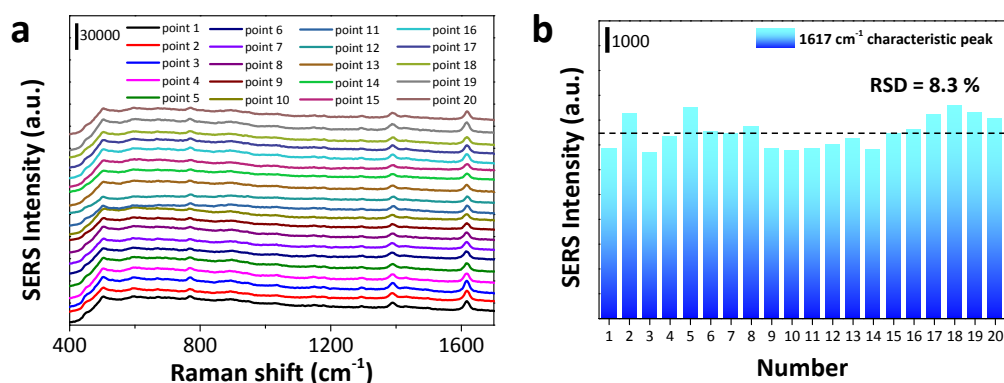


Fig. S13 (a) SERS spectra (at 633 nm) of 20 individual tips of AuMNs_[16 ppm]. (b) RSD value of SERS intensity at 1617 cm^{-1} characteristic peak from the 20 SERS spectra in (a).

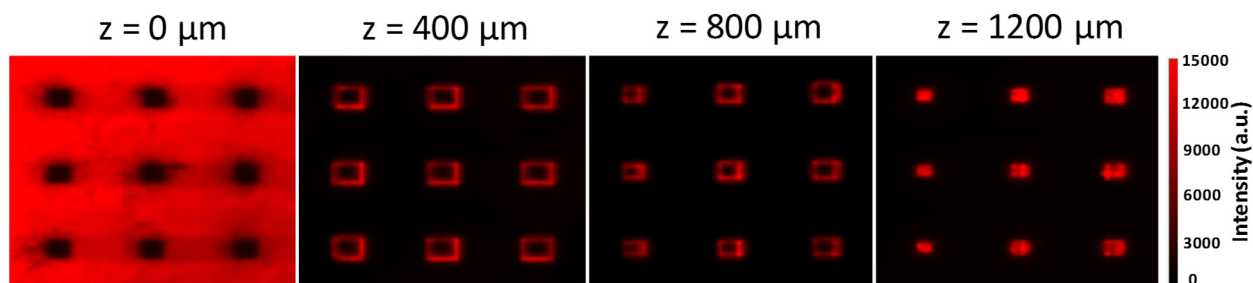


Fig. S14 The SERS images (at 785 nm) within 3×3 microneedles of AuMNs-MB_[16 ppm] at $z = 0 \text{ μm}$, 400 μm , 800 μm , and 1200 μm of heights.

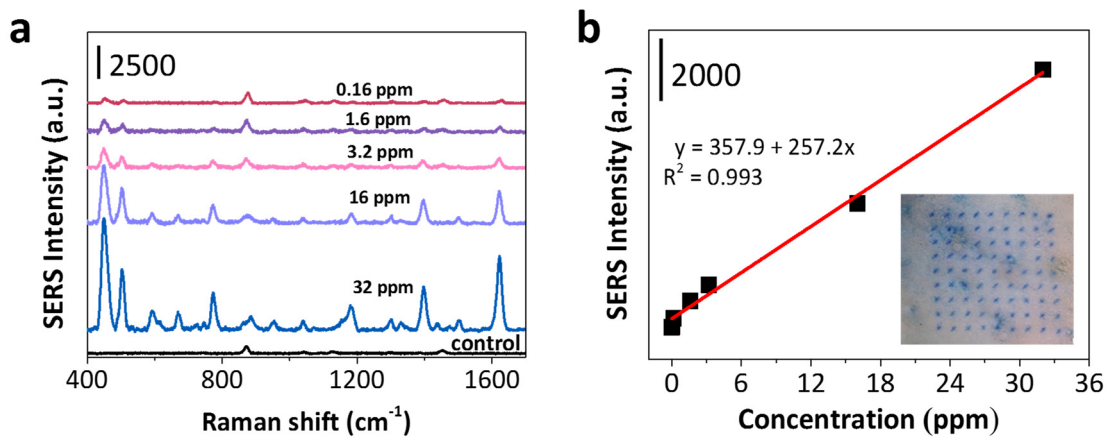


Fig. S15 (a) Backside-excitation SERS spectra of AuMNs-MB with different concentrations of MB punctured into pigskin and its (b) corresponding concentration linearity of SERS intensity with varying MB concentration (Inset: photograph of AuMNs-MB punctured into pigskin).

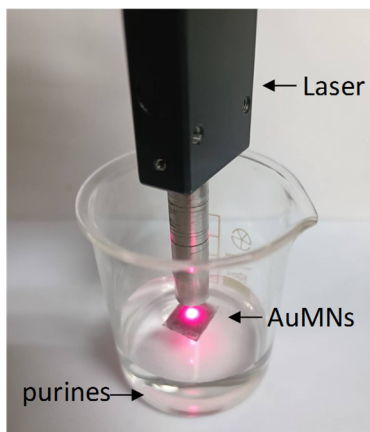


Fig. S16 Photograph of backside-excitation SERS measurement for solution sample detection.

The decrease of ABDA absorbance (at 360, 380, and 400 nm) upon increasing irradiation of 650 nm laser demonstrated the increased yield of $^1\text{O}_2$ (Fig. S18a).² Moreover, AuMNs-MB_[16 ppm] with 20 min of 650 nm-light excitation gave rise to a 1:1:1 triplet signal of $^1\text{O}_2$ spin trapper TEMP, showing direct evidence for the $^1\text{O}_2$ generation.³

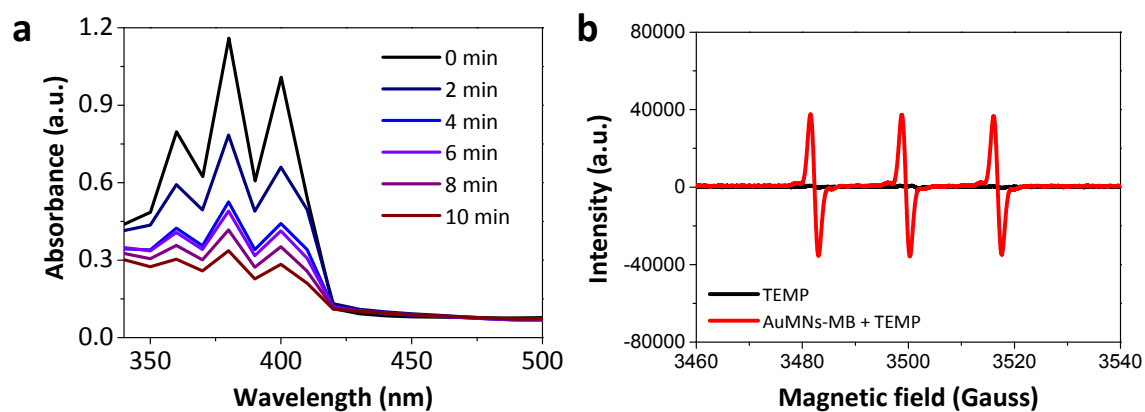


Fig. S17 (a) Absorption spectra of ABDA within 10 min of irradiation with a 650 nm laser. (b) ESR spectra of TEMP before and after the treatment of AuMNs-MB_[16 ppm] with 20 min of a 650 nm-light excitation.

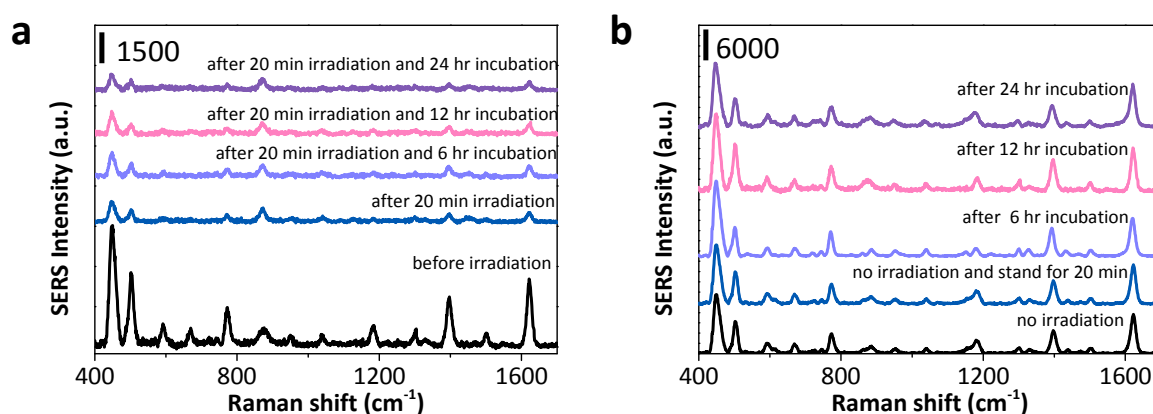


Fig. S18 SERS spectra of AuMNs-MB_[16 ppm] with *S. aureus* (10^2 CFU/cm²) seeded on agarose medium (a) before/after 20 min of 650 nm laser irradiation, (b) no irradiation and subsequent incubation.

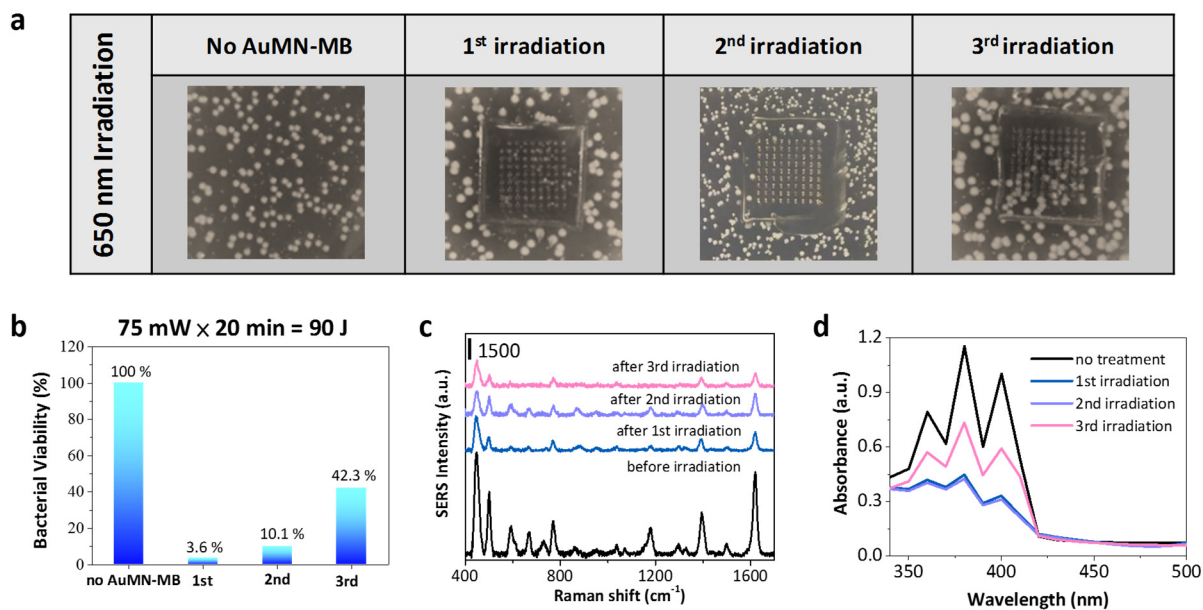


Fig. S19 (a) Photographs of bacterial colonization, (b) quantitation of bacterial viability, (c) SERS spectra of the same AuMNs-MB_[16 ppm] with *S. aureus* (5×10^2 CFU/cm²) seeded on individual agarose medium before/after the 1st, 2nd, and 3rd irradiation cycles with a 650 nm laser at 90 J (75 mW and for 20 min). (d) Absorption of ABDA with no treatment and AuMNs-MB_[16 ppm] after the 1st, 2nd, and 3rd irradiation cycles with a 650 nm laser for 20 min.

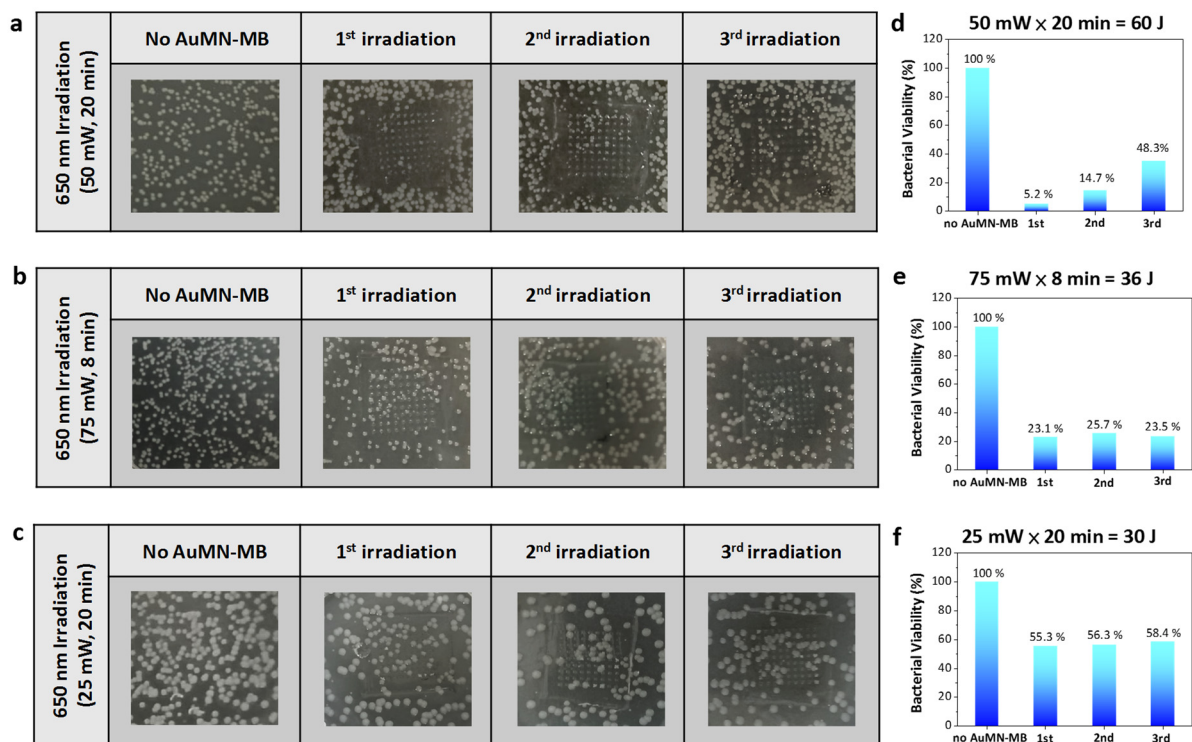


Fig. S20 Photographs of bacterial colonization after the 1st, 2nd, and 3rd irradiation cycles with a 650 nm laser at (a) 60 J (50 mW and 20 min), (b) 36 J (75 mW and 8 min), and (c) 30 J (25 mW and 20 min). The corresponding bacterial viabilities are represented in (d) a, (e) b, and (f) c.

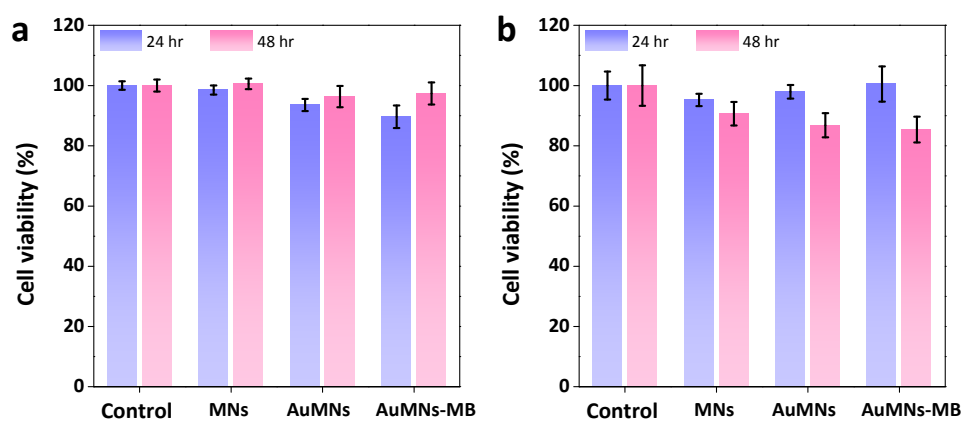


Fig. S21 Cell viability of (a) THP-1 (cells suspended on MNs) and (b) 3T3 fibroblast cells (cells adhered on MNs) with MNs, AuMNs, and AuMNs-MB_[16 ppm] treatments by using the CCK-8 assay after 24 and 48 h of incubation.

References

1. M. -M. Shi, D. Bao, B. -R. Wulan, Y. -H. Li, Y. -F. Zhang, J. -M. Yan and Q. Jiang, *Adv. Mater.*, 2017, 29, 1606550.
2. I. Roy, T. Y. Ohulchanskyy, H. E. Pudavar, E. J. Bergey, A. R. Oseroff, J. Morgan, T. J. Dougherty and P. N. Prasad, *J. Am. Chem. Soc.*, 2003, 125, 7860.
3. M. L. Marin, L. Santos-Juanes, A. Arques, A. M. Amat and M. A. Miranda, *Chem. Rev.*, 2012, 112, 1710.